

# Magnetic susceptibility anisotropies in a two-dimensional quantum Heisenberg antiferromagnet with Dzyaloshinskii-Moriya interactions

M. B. Silva Neto,<sup>1,\*</sup> L. Benfatto,<sup>2</sup> V. Juricic,<sup>1</sup> and C. Morais Smith<sup>1</sup>

<sup>1</sup>*Institute for Theoretical Physics, University of Utrecht,  
P.O. Box 80.195, 3508 TD, Utrecht, The Netherlands*

<sup>2</sup>*SMC-INFN and Department of Physics, University of Rome "La Sapienza",  
Piazzale Aldo Moro 5, 00185, Rome, Italy*

(Dated: November 7, 2018)

The magnetic and thermodynamic properties of the two-dimensional (2D) quantum Heisenberg antiferromagnet (QHAF) that incorporates both a Dzyaloshinskii-Moriya (DM) and pseudo-dipolar (XY) interactions are studied within the framework of a generalized nonlinear sigma model (NLSM). We calculate the static uniform susceptibility and sublattice magnetization as a function of temperature and we show that: i) the magnetic-response is anisotropic and differs qualitatively from the expected behavior of a conventional easy-axis QHAF; ii) the Néel second-order phase transition becomes a crossover, for a magnetic field  $B \perp \text{CuO}_2$  layers. We provide a simple and clear explanation for all the recently reported *unusual* magnetic anisotropies in the low-field susceptibility of  $\text{La}_2\text{CuO}_4$ , L. N. Lavrov *et al.*, Phys. Rev. Lett. **87**, 017007 (2001), and we demonstrate explicitly why  $\text{La}_2\text{CuO}_4$  can not be classified as an ordinary easy-axis antiferromagnet.

PACS numbers: 74.25.Ha, 75.10.Jm, 75.30.Cr

## I. INTRODUCTION

The usual starting point for the description of the magnetism in undoped cuprates is the 2D isotropic Heisenberg model

$$H = J \sum_{\langle ij \rangle} \mathbf{S}_i \cdot \mathbf{S}_j, \quad (1)$$

with only the AF super-exchange  $J$  between the nearest-neighbor Cu<sup>++</sup> spins,  $\mathbf{S}_i$ .<sup>1</sup> Remarkably, a long-wavelength NLSM description of such model has been shown to correctly capture many of the features observed experimentally in the high-temperature paramagnetic phase.<sup>2,3</sup> At lower temperatures, however, small anisotropies like the DM and XY interactions become important, and the commonly used isotropic description is no longer adequate to describe the long-wavelength magnetic properties of  $\text{La}_2\text{CuO}_4$ . In a recent paper, Lavrov *et al.* reported on some *unusual* anisotropies in the low-field magnetic susceptibility observed in detwinned  $\text{La}_2\text{CuO}_4$  single crystals.<sup>4</sup> Among the unexpected features one could mention: i) an almost featureless transverse in-plane susceptibility,  $\chi_a$ , for an extended temperature range; ii) the increase of the longitudinal susceptibility,  $\chi_b$ , as one approaches the Néel transition temperature,  $T_N$ , from the ordered side; iii) the anomalous  $T = 0$  hierarchy  $\chi_c > \chi_b > \chi_a$ , where  $a, b, c$  represent the low-temperature orthorhombic (LTO) crystallographic directions of Fig. 1.

In this article we investigate theoretically the magnetic response and thermodynamic properties of the square-lattice QHAF that incorporates both the DM and XY anisotropy terms by investigating the generalized NLSM corresponding to this microscopic problem. As it has been stressed in the context of one-dimensional systems,<sup>5</sup>

the DM term generates an effective staggered magnetic field proportional to the applied uniform field. In the two-dimensional case the continuum field theory allows one to reproduce straightforwardly the same effect,<sup>6,7</sup>. In Ref.<sup>7</sup> the attention was focused on the (classical) spin configurations expected in an external field. In this paper we investigate instead the thermodynamical properties of the system, which enter in a crucial way in the evaluation of the static uniform susceptibility,  $\chi$ , as a function of temperature,  $T$ . In particular, we show that the coupling induced by the DM term between the magnetic field and the antiferromagnetic order parameter is particularly relevant when the order-parameter fluctuations become critical, leading to an anomalous magnetic response of the system, as observed for example in<sup>4</sup>. As an outcome of our studies we observe that, while the isotropic nonlinear sigma model (NLSM) is well established to give a proper description of the magnetism in the high-temperature paramagnetic phase,  $T \gg T_N$ ,<sup>2,3</sup> for the ordered (broken) phase,  $T < T_N$ , we find more appropriate the adoption of a *soft* version of such fixed-length constraint, in order to correctly capture the physics of the longitudinal fluctuations. For the sake of clarity, we refer explicitly to the  $\text{La}_2\text{CuO}_4$  system throughout the paper, but the results presented here apply to any 2D square-lattice QHAF where the DM and/or XY anisotropy interactions are present, as for example other cuprates and nickelates  $\text{La}_2\text{NiO}_4$ .<sup>8</sup>

## II. THE LONG-WAVELENGTH LIMIT

We consider the following square-lattice single-layer  $S = 1/2$  Hamiltonian for the  $\text{La}_2\text{CuO}_4$  system

$$H = J \sum_{\langle i,j \rangle} \mathbf{S}_i \cdot \mathbf{S}_j + \sum_{\langle i,j \rangle} \mathbf{D}_{ij} \cdot (\mathbf{S}_i \times \mathbf{S}_j) + \sum_{\langle i,j \rangle} \mathbf{S}_i \cdot \overleftrightarrow{\Gamma}_{ij} \cdot \mathbf{S}_j, \quad (2)$$

where  $\mathbf{D}_{ij}$  and  $\overleftrightarrow{\Gamma}_{ij}$  are, respectively, the DM and XY anisotropic interaction terms that arise due to the spin-orbit coupling and direct-exchange in the low-temperature orthorhombic (LTO) phase of  $\text{La}_2\text{CuO}_4$ .<sup>8</sup> The direction and the alternating pattern of the DM vectors, shown in Fig. 1, are a direct consequence of the tilting structure of the oxygen octahedra and of the symmetry of the  $\text{La}_2\text{CuO}_4$  crystal. Throughout this work we adopt the LTO (*bac*) coordinate system of Fig. 1, for both the spin and lattice degrees of freedom, and we use units where  $\hbar = k_B = 1$ . Thus we have that

$$\mathbf{D}_{ij} = \frac{1}{\sqrt{2}}(-d, d, 0), \quad \mathbf{D}_{ik} = \frac{1}{\sqrt{2}}(d, d, 0), \quad (3)$$

and

$$\overleftrightarrow{\Gamma}_{ij} = \begin{pmatrix} \Gamma_1 & \Gamma_2 & 0 \\ \Gamma_2 & \Gamma_1 & 0 \\ 0 & 0 & \Gamma_3 \end{pmatrix}, \quad \overleftrightarrow{\Gamma}_{ik} = \begin{pmatrix} \Gamma_1 & -\Gamma_2 & 0 \\ -\Gamma_2 & \Gamma_1 & 0 \\ 0 & 0 & \Gamma_3 \end{pmatrix},$$

where  $ij$  and  $ik$  label the  $\text{Cu}^{++}$  sites (see Fig. 1), and  $d$  and  $\Gamma_{1,2,3} > 0$  are of order  $10^{-2}$  and  $10^{-4}$ , respectively, in units of  $J$ .<sup>8</sup>

To construct the long wavelength effective theory for the above Hamiltonian we follow the standard procedure: we write

$$\frac{\mathbf{S}_i(\tau)}{S} = e^{i\mathbf{Q} \cdot \mathbf{x}_i} \mathbf{n}(\mathbf{x}_i, \tau) + \mathbf{L}(\mathbf{x}_i, \tau), \quad (4)$$

where  $\mathbf{n}$  and  $\mathbf{L}$  are, respectively, the staggered and uniform components of the spin and  $\mathbf{Q} = (\pi, \pi)$ . We then integrate out  $\mathbf{L}$  and we obtain a modified NLSM where additional terms appear due to the DM and XY interactions ( $\beta = 1/T$ ) and

$$S = \frac{1}{2g_0c_0} \int_0^\beta d\tau \int d^2\mathbf{x} \{ (\partial_\tau \mathbf{n})^2 + c_0^2 (\nabla \mathbf{n})^2 + (\mathbf{D}_+ \cdot \mathbf{n})^2 + \Gamma_c n_c^2 \}, \quad (5)$$

and the fixed length constraint  $\mathbf{n}^2 = 1$  is implicit (see also Ref.<sup>6,7</sup>). Here  $g_0$  is the bare coupling constant, related to the spin-wave velocity,  $c_0$ , and renormalized stiffness,  $\rho_s$ , through  $\rho_s = c_0(1/Ng_0 - \Lambda/4\pi)$ ,<sup>2,3</sup> where  $\Lambda$  is a cutoff for momentum integrals (we set the lattice spacing  $a = 1$ ) and  $N = 3$  is the number of spin components. Finally,

$$\mathbf{D}_+ = 2S(\mathbf{D}_{ij} + \mathbf{D}_{ik}), \quad (6)$$

see Fig. 1, and

$$\Gamma_c = 32JS^2(\Gamma_1 - \Gamma_3) > 0, \quad (7)$$

and we neglected a small anisotropic correction to  $c$  coming from the XY term, since  $\Gamma_{1,2} \ll J$ .

Observe that in the NLSM (5) only the sum of the DM and XY terms on the  $(ij)$  and  $(ik)$  bonds appears. This has several consequences: (i) the XY term generates a contribution to (5) proportional to  $-\Gamma_{\alpha\alpha} n_\alpha^2$ ,  $\alpha = a, b, c$ , where  $\Gamma_{\alpha\beta} = (1/2)(\Gamma_{ij} + \Gamma_{ik})_{\alpha\beta} = \text{diag}(\Gamma_1, \Gamma_1, \Gamma_3)$ . Since  $\mathbf{n}^2 = 1$ , such contribution reduces to a constant shift in the classical energy plus the  $\Gamma_c n_c^2$  term in Eq. (5). This allows us to identify the  $ab$  as the first easy plane. The property that only the combination  $\Gamma_1 - \Gamma_3$  affects the physics of the model (2) was an outcome of the numerical results of the RPA improved spin-wave analysis of Ref.<sup>9</sup>, but no explanation for this effect was provided. (ii) The DM distortion enters the action (5) only through the vector  $\mathbf{D}_+ = D_+ \hat{\mathbf{x}}_a$  ( $\hat{\mathbf{x}}_a, \hat{\mathbf{x}}_b$ , and  $\hat{\mathbf{x}}_c$  are the LTO

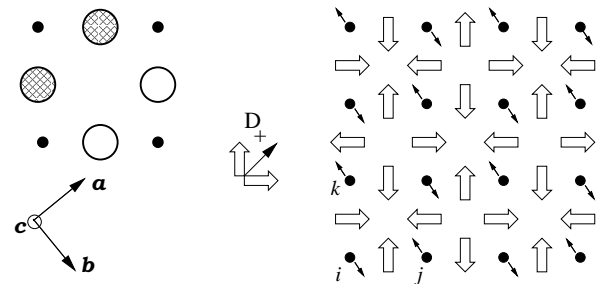


FIG. 1: Left: the hatched circles represent the  $\text{O}^{2-}$  ions tilted above the  $\text{CuO}_2$  plane; the empty ones are tilted below it; small black circles are  $\text{Cu}^{++}$  ions; *bac* orthorhombic coordinate system. Right: Schematic arrangement of the staggered magnetization (small black arrows) and DM vectors (open arrows). Center: continuum definition of  $\mathbf{D}_+$ .

unit vectors), rendering  $bc$  a second easy plane. When the system orders we find the staggered magnetization at  $\langle \mathbf{n} \rangle = \sigma_0 \hat{\mathbf{x}}_b$ , as observed experimentally,<sup>10</sup> because the orientation along  $\hat{\mathbf{x}}_a$  or  $\hat{\mathbf{x}}_c$  would cost an energy  $D_+^2$  or  $\Gamma_c$ , respectively. Moreover, since the uniform magnetization is given by<sup>6,7</sup>

$$\langle \mathbf{L} \rangle = \frac{1}{2J} \langle (\mathbf{n}) \times \mathbf{D}_+ \rangle, \quad (8)$$

we find that, in the AF phase,  $\langle \mathbf{L} \rangle$ , is directed along  $\hat{\mathbf{x}}_c$ ,

so that the  $\text{Cu}^{++}$  spins are canted out of the  $ab$  plane and confined to the  $bc$  plane.

### III. MAGNETIC SUSCEPTIBILITY

To evaluate the static uniform susceptibility,  $\chi_\alpha$ , we rederive from the microscopic Hamiltonian (2) the quantum action (5) in the presence of a magnetic field  $\mathbf{B}$  (in units of  $g_S\mu_B/\hbar = 1$ , where  $g_S \approx 2$  is the gyromagnetic ratio and  $\mu_B$  is the Bohr magneton)<sup>6,7</sup>

$$\mathcal{S}(\mathbf{B}) = \mathcal{S}(\partial_\tau \mathbf{n} \rightarrow \partial_\tau \mathbf{n} + i\mathbf{B} \times \mathbf{n}) + \frac{1}{g_0 c_0} \int_0^\beta d\tau \int d^2\mathbf{x} \mathbf{B} \cdot (\mathbf{D}_+ \times \mathbf{n}). \quad (9)$$

The last term in the above equation, which couples the DM vector  $\mathbf{D}_+$  and the staggered magnetization  $\mathbf{n}$ , is responsible for many of the *unusual* features observed experimentally in  $\text{La}_2\text{CuO}_4$ . However, this coupling is generic to any square-lattice system, as other cuprates and nickelates, where symmetry guarantees that the DM vectors alternate in sign between neighboring bonds.<sup>8</sup>

The *zero-field* magnetic susceptibility is calculated in linear response theory as

$$\chi_\alpha = \frac{1}{\beta V} \left. \frac{\partial^2 \log Z}{\partial B_\alpha^2} \right|_{B=0}, \quad (10)$$

where  $Z(\mathbf{B}) = \int \mathcal{D}\mathbf{n} \exp\{-\mathcal{S}(\mathbf{B})\}$  is the Euclidean partition function for the action (9), and we obtain

$$\begin{aligned} \chi_a &= \chi_a^u + \frac{\sigma_0^2}{g_0 c_0}, \\ \chi_b &= \chi_b^u + \frac{D_+^2}{g_0 c_0} G_c(0, 0), \\ \chi_c &= \chi_c^u + \frac{\sigma_0^2}{g_0 c_0} + \frac{D_+^2}{g_0 c_0} G_b(0, 0), \end{aligned} \quad (11)$$

where

$$G_\alpha^{-1}(\mathbf{k}, \omega_n) = c_0^2 \mathbf{k}^2 + \omega_n^2 + M_\alpha^2 \quad (12)$$

is the inverse propagator for the magnetic modes  $a, b, c$ , with gaps  $M_\alpha$  and

$$\chi_\alpha^u = \frac{1}{\beta V} \sum_{q=(\mathbf{k}, \omega_n)} \{G_\beta(q) + G_\gamma(q) - 4\omega_n^2 G_\beta(q) G_\gamma(q)\}, \quad (13)$$

is the traditional ‘‘uniform’’ contribution to the susceptibility, with  $(\alpha\beta\gamma) = (abc)$  and its permutations.

The set of Eqs. (11), following from the quantum actions (5) and (9), is the main results of this article. A few remarks are in order now concerning the usefulness of the NLSM approach to the model (2) with respect to other approaches.<sup>8,9,11</sup> First, the action (9) allows one to easily track down the source of the anisotropic magnetic response, as coming from the term  $\mathbf{B} \cdot (\mathbf{D}_+ \times \mathbf{n})$ . In fact,

depending on the directions of  $\mathbf{D}_+$  and of the applied field, there will be (or not) additional terms proportional to  $G_\alpha$  in Eq. (11), responsible for the *unusual* magnetic response. Second, this coupling is generic to any system where the lack of inversion-center symmetry allows for an oscillating DM interaction between neighboring spins. Third, Eqs. (11) are *exact*, within linear response theory, even though the evaluation of the zero-field thermodynamic quantities  $\sigma_0(T)$  and  $M_\alpha(T)$  will require, in general, a certain degree of approximation. Nevertheless, we show now that all the qualitative features observed in<sup>4</sup> are already present at the mean-field level.

The thermodynamic properties of the model (5) can be investigated by means of a large- $N$  expansion.<sup>3</sup> At  $N = \infty$ , and for  $T > T_N$ , we find  $\sigma_0 = 0$  and

$$M_b^2 = c_0^2 \xi^{-2}, \quad M_a^2 = D_+^2 + c_0^2 \xi^{-2}, \quad M_c^2 = \Gamma_c + c_0^2 \xi^{-2}, \quad (14)$$

where the correlation length,  $\xi$ , is calculated through an *averaged* constraint equation  $1 = NI_\perp(\xi)$ . Here  $I_\perp = (1/2)(I_a + I_c)$  with

$$I_\alpha = \frac{g_0 c_0}{\beta V} \sum_{\mathbf{k}, \omega_n} G_\alpha(\mathbf{k}, \omega_n) = \frac{g_0 T}{2\pi c_0} \log \left\{ \frac{\sinh(c_0 \Lambda / 2T)}{\sinh(M_\alpha / 2T)} \right\}. \quad (15)$$

Since both transverse spin-wave modes,  $a$  and  $c$ , are gapped, the 2D system orders at a finite Néel temperature,  $T_N$ , defined by  $1 = NI_\perp(\xi = \infty)$ .<sup>12</sup>

For the ordered phase,  $T < T_N$ , instead of replacing the local constraint by an *average* one, we introduce a potential of the type  $(u_0/2)(\mathbf{n}^2 - 1)^2$  in the action (5), making the constraint locally *soft*. In this case we obtain a generalized *linear* sigma model (LSM), which leads to an ordered phase described by:

$$\sigma_0^2 = 1 - NI_\perp, \quad M_b^2 = 2\sigma_0^2 u_0, \quad M_a^2 = D_+^2, \quad M_c^2 = \Gamma_c. \quad (16)$$

We should emphasize that the only new parameter here is the energy scale  $u_0 = (\gamma J)^2$ , where  $\gamma$  is a fitting parameter that will be fixed later through comparison with experiments. However, an inspection of Eq. (16), indicates that neither  $T_N$  nor the values of  $\sigma_0$  and  $M_{a,c}$  depend on  $u_0$ . The only difference is the physics of the longitudinal fluctuations, for  $T < T_N$ . While the hard constraint yields a longitudinal mode always gapless,<sup>13</sup> the soft one gives a mass for the longitudinal mode below  $T_N$  that is proportional to the strength of the order parameter.

We fix the large- $N$  parameters for  $\text{La}_2\text{CuO}_4$  by comparing the correlation length,  $\xi$ , with the experimental data in the paramagnetic phase, and we use  $M_a(T = 0) \equiv D_+ = 2.5$  meV and  $M_c(T = 0) \equiv \sqrt{\Gamma_c} = 5.0$  meV, for the zone center in-plane and out-of-plane spin-wave gaps as determined from neutron scattering.<sup>14</sup> In the inset (a) of Fig. 2 we compare  $\xi^{-1}$  obtained for  $\rho_s = 0.1J$ ,  $c_0 = 1.3J$  and  $J = 100$  meV with the curve  $\xi_{exp}$ , which represents the best fit of the experimental data at  $T > T_N$  obtained in the isotropic NLSM<sup>15</sup> (so that  $\xi_{exp}^{-1}$  deviates

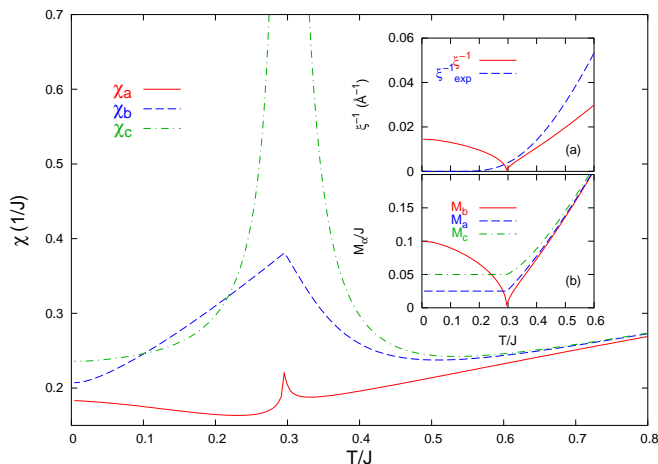


FIG. 2: (Color online) Temperature dependence of the magnetic susceptibilities  $\chi_a$ ,  $\chi_b$  and  $\chi_c$  from (11). Insets: (a) temperature dependence of  $M_{a,b,c}$  and (b)  $\xi^{-1}$ .

from the experimental data near  $T_N$ ). When  $1/N$  corrections to our calculations are included one expects that the ratio  $T_N/J$  is reduced,<sup>13</sup> which allows for larger and more realistic values for  $\rho_s$ ,  $c_0$ , and  $J$ .<sup>2,3</sup> Nevertheless, with the above parameters we find  $\sigma_0(T=0) \approx 0.46$  which leads to an effective moment of the  $\text{Cu}^{++}$  spins,  $\mu = g_s S \sigma_0 \mu_B \approx 0.46 \mu_B$ , in good agreement with the experiments.<sup>15</sup> The resulting  $M_{a,b,c}$  as a function of temperature are shown in the inset (b) of Fig. 2 for  $\gamma = 0.15$ , a choice that will be justified below.

### A. Temperature dependence of $\chi_a$ , $\chi_b$ and $\chi_c$

Let us now discuss how all the unusual features of the susceptibilities reported in<sup>4</sup> follow straightforwardly from Eqs. (11) already at the mean-field (large  $N$ ) level (see Fig. 2). At large temperatures,  $T \gg T_N$ , all three  $\chi_{a,b,c}$  exhibit the usual linear- $T$  behavior observed experimentally<sup>16</sup> and expected for the uniform susceptibility of the isotropic NLSM.<sup>3</sup> As  $T \rightarrow 0$ , on the other hand,  $\chi_b^u \rightarrow 0$  while both  $\chi_c^u$  and  $\chi_a^u$  saturate at very small, but nonzero, values. The smooth evolution through the transition experimentally observed in  $\chi_a$  is due to the fact that  $\chi_a^u$  contains terms like  $I_a$  in Eq. (15), which are regular for the transverse modes (always gapped by the DM and XY interactions) and diverge logarithmically at  $T_N$  for the longitudinal mode as  $M_b(T \rightarrow T_N) \rightarrow 0$ . This divergence appears as a hump in the numerical evaluation of  $\chi_a$  presented in Fig. 2 and is an artifact of both the low dimensionality and of the large- $N$  limit (a coupling between  $\text{CuO}_2$  layers or a nonzero anomalous dimension  $\eta$  for the propagator of the longitudinal mode regulates such logarithmic infrared divergence of  $I_b$  at  $T_N$  and wipes out the feature in  $\chi_a$ ). Finally, the weak increase observed in  $\chi_a$  as  $T \rightarrow 0$ , also observed experimentally, is due to the compensation be-

tween the decrease of  $\chi_a^u$  and the increase of the term  $\sigma_0^2/g_0c_0$ .

We turn now to  $\chi_c$  and  $\chi_b$ . As  $T \rightarrow T_N$ ,

$$\chi_c \approx \frac{D_+^2}{g_0c_0} G_b(0,0) = \frac{D_+^2}{g_0c_0} \frac{1}{M_b^2} \quad (17)$$

diverges because of the vanishing of the mass of the longitudinal mode,  $M_b(T \rightarrow T_N^+) \rightarrow 0$ , and this is associated with the ferromagnetic ordering of the canted moments.<sup>11</sup> It is essential to have a finite  $M_b$  below  $T_N$  in order to correctly reproduce the behavior of  $\chi_c$  in the ordered phase. So, although the hard-spin model correctly reproduces the vanishing of  $M_b$  as  $T \rightarrow T_N^+$ , it is not adequate for the ordered phase, where  $M_b = 0$  leading to a diverging  $\chi_c$  for all  $T < T_N$ . That is why we have adopted the soft version of the constraint below  $T_N$ .

Finally, we observe in Fig. 2 that  $\chi_b$  is not divergent at  $T_N$  but exhibits a well pronounced peak. This is a consequence of the term  $D_+^2 G_c(0,0)/g_0c_0 = D_+^2/(g_0c_0 M_c^2)$ . According to Eq. (14), as we approach  $T_N$  from the paramagnetic side  $\xi^{-2}$  goes to zero and  $D_+^2/(g_0c_0 M_c^2)$  approaches the value  $D_+^2/(g_0c_0 \Gamma_c) \approx 1/(4g_0c_0)$ , which is controlled by the ratio between the DM and XY interaction terms. Observe that the absence of a similar feature in  $\chi_a$  is due to the fact that, for  $\mathbf{B} \parallel a$ ,  $\mathbf{B} \cdot (\mathbf{D}_+ \times \mathbf{n}) = 0$ , so  $\chi_a$  has only the uniform contribution  $\chi_a^u$ . Thus, the increase in  $\chi_b$  as  $T \rightarrow T_N^-$  is clearly a result of the sum of its uniform part,  $\chi_b^u$ , which is monotonically increasing with  $T$ , and the term  $D_+^2/(g_0c_0 M_c^2)$ , which is constant below  $T_N$  and decreases instead as  $\sim \xi^2$  above  $T_N$ .

### B. Unusual $\chi_a(0) < \chi_b(0) < \chi_c(0)$ hierarchy

A comment is in order now concerning the hierarchy of the  $T=0$  susceptibilities in Fig. 2. For an ordinary easy-axis AF with different in-plane and out-of-plane transverse gaps,  $M_a < M_c$ , it is expected that the  $T=0$  *uniform* susceptibilities should satisfy  $\chi_b^u(0) < \chi_a^u(0) < \chi_c^u(0)$ , with the lowest value for the easy axis and with a transverse susceptibility smaller in the direction of the smaller gap. This is in fact the result that one obtains after dropping the terms proportional to  $D_+^2$  in Eq. (11). However, the unusual coupling between  $\mathbf{B}$  and  $\mathbf{n}$  in (9) gives rise to the terms proportional to  $D_+^2$  in  $\chi_b(0)$  and  $\chi_c(0)$ , which, in turn, lead to the following  $T=0$  values for the three susceptibilities

$$\chi_a \approx \frac{\sigma_0^2}{g_0c_0}, \quad \chi_b = \frac{1}{g_0c_0} \frac{D_+^2}{M_c^2}, \quad \chi_c \approx \chi_a + \frac{1}{g_0c_0} \frac{D_+^2}{M_b^2}, \quad (18)$$

resulting in the *unusual* hierarchy of the zero-temperature values and rendering  $\text{La}_2\text{CuO}_4$  an example of an unconventional easy-axis antiferromagnet. Observe that  $\chi_c(0)/\chi_a(0) > 1$  always, and we use the  $T=0$  intercept of  $\chi_c$  to fix  $\gamma = 0.15$ . Finally, for our choice of parameters the ratio  $\chi_b(0)/\chi_a(0) \sim 1.1$ , in relatively

good agreement with the experiments,<sup>4</sup> but it depends in general on the values of the transverse masses.<sup>17</sup>

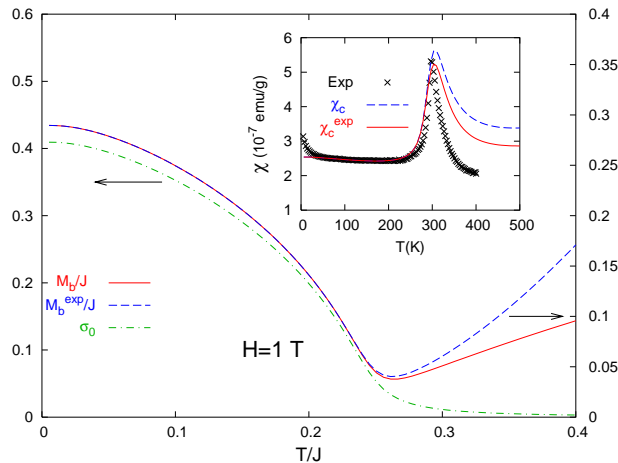


FIG. 3: (Color online) Plot of  $\sigma_0$ ,  $M_b$ , and  $M_b^{exp}$  from Eqs. (21) and (20).  $M_b^{exp}$  is fitted to the experimental data for the inverse correlation length above  $T_N$ , see discussion in the text below Eq. (21). Inset:  $\chi_c$  in units of emu/g and experimental points from<sup>4</sup>.  $\chi_c^{exp}$  is obtained from Eqs. (11) using  $M_b^{exp}$ . Here  $\rho_s = 0.07J$ ,  $\gamma = 0.5$ ,  $a = 5.3 \text{ \AA}$ , the out-of-plane lattice parameter  $d = 13.5 \text{ \AA}$ , and we added a  $T$ -independent shift of  $\chi_{vV} \approx 1.0 \times 10^{-7} \text{ emu/g}$  to account for the van Vleck paramagnetic susceptibility.<sup>4</sup>

#### IV. EFFECTS OF A FINITE MAGNETIC FIELD $\mathbf{B} \perp \text{CuO}_2$ LAYERS

The result for  $\chi_c$  plotted in Fig. 2 can be further improved by considering explicitly the nontrivial effects of the combination  $\mathbf{B} \perp ab$  plane and  $\mathbf{D}_+ \neq 0$  on the thermodynamic properties of the theory (9). In fact, in this case the last term in Eq. (9) becomes  $-(1/g_0 c_0) \int h n_b$ , where  $h = |\mathbf{B} \times \mathbf{D}_+|$ . Within the NLSM formulation the averaged constraint equation defines a self-consistency equation for the order parameter given by:

$$\sigma_0^2 = 1 - NI_{\perp}(M_{\perp}^2 + h/\sigma_0) \quad (19)$$

where the masses appearing in the transverse spin fluctuations (15) are themselves a function of  $\sigma_0$ :

$$M_a^2 = D_+^2 + \frac{\hbar}{\sigma_0}, \quad M_c^2 = \Gamma_c + \frac{\hbar}{\sigma_0} + B^2. \quad (20)$$

As one can see, besides a (quantitatively small) hardening of the  $c$  mode due to the applied field, we find that the term  $h/\sigma_0$  plays a role similar to the correlation length,  $c^2 \xi^{-2}$ , in Eq. (14). The result is that  $\sigma_0$  never vanishes for  $h \neq 0$  (see Fig. 3), and because of the DM interaction, a nonvanishing  $\mathbf{B} \perp ab$  plane transforms the Néel second order phase transition into a crossover. In analogy with the discussion of the case  $\mathbf{B} = 0$ , the

proper description of the longitudinal-field fluctuations below the crossover temperature can be done within the LSM, where the order-parameter equation and the longitudinal mass read:

$$u_0 \sigma_0 (\sigma_0^2 - 1 + NI_{\perp}(M_{\perp}^2 + h/\sigma_0, T)) = h, \quad M_b^2 = 2u_0 \sigma_0^2 + \frac{\hbar}{\sigma_0}. \quad (21)$$

Observe that the crossover temperature obtained from Eq. (19) and Eq. (21) is almost the same. To interpolate between the two solutions we define  $(M_b^{exp})^2 = \max(h/\sigma_0, 2u_0 \sigma_0^2 + h/\sigma_0)$  and we fix the parameter values by fitting  $M_b^{exp}$  to the experimental data on the correlation length above  $T_N$ . As far as the  $c$ -axis susceptibility is concerned it is now evident from the inset of Fig. 3 that  $\chi_c$  no longer diverges ( $M_b$  is always finite) but becomes peaked at a crossover temperature at which  $M_b$  has a minimum (see Fig. 3). Observe also that for  $\chi_a$  and  $\chi_c$  the effects of a finite magnetic field are instead negligible, leading only to small quantitative differences with respect to the calculation presented before for  $\mathbf{B} = 0$ .

#### V. CONCLUSIONS

In conclusion, we have derived the uniform magnetic susceptibility within the long-wavelength effective theory (5)-(9) for the single-layer square-lattice QHAF with DM and XY interactions (2). We obtained that the magnetic response is anisotropic, in remarkable agreement with the experiments of<sup>4</sup>, and differs from the expected behavior for a more conventional easy-axis QHAF. Due to the presence of the DM term, the uniform magnetic field generates an effective staggered field proportional to both the DM interaction and to the applied field. We showed that the coupling between the magnetic field and the staggered order parameter is particularly relevant when the order-parameter fluctuations become critical, leading to an anomalous magnetic response of the system, as observed for example in<sup>4</sup>. Moreover, this same coupling is responsible for the unusual zero temperature hierarchy of the susceptibilities, rendering  $\text{La}_2\text{CuO}_4$  an example of an unconventional easy-axis antiferromagnet. Finally, we considered the effect of a finite magnetic field on the  $\chi_c$  susceptibility. We found that, for a nonzero  $\mathbf{B} \perp ab$  plane, the Néel second order phase transition becomes a crossover, see Fig. 3, in analogy with the behavior of a ferromagnet in a finite magnetic field. The finite-field effects are instead irrelevant as far as the susceptibilities in the  $a$  and  $b$  direction are considered. However, the case of  $\mathbf{B} \parallel b$  presents interesting outcomes as far as the selection rules for one-magnon Raman scattering are concerned, as it has been discussed recently in Ref.<sup>18</sup>. While Eq. (9) and (11) have been derived for the case of  $\text{La}_2\text{CuO}_4$  materials, the present analysis can be extended to other QHAF systems where the lack of inversion-center symmetry allows for an oscillating DM interaction between neighboring spins.

## VI. ACKNOWLEDGEMENTS

The authors have benefitted from discussions with A. Aharony, Y. Ando, B. Binz, C. Castellani, A. H. Cas-

tro Neto, and R. Gooding. We also thank A. Lavrov, for fruitful discussions and for providing us with the experimental data for  $\chi_c$  from<sup>4</sup>, shown in Fig. 3 (inset).

- 
- \* Electronic address: barbosa@phys.uu.nl
- <sup>1</sup> M. A. Kastner, R. J. Birgeneau, G. Shirane, and Y. Endoh, *Rev. Mod. Phys.* **70**, 897 (1998).
  - <sup>2</sup> S. Chakravarty, B. I. Halperin, and D. R. Nelson, *Phys. Rev. B* **39**, 2344 (1989).
  - <sup>3</sup> A. V. Chubukov, S. Sachdev, and J. Ye, *Phys. Rev. B* **49**, 11919 (1994).
  - <sup>4</sup> A. N. Lavrov, Y. Ando, S. Komiya, and I. Tsukada, *Phys. Rev. Lett.* **87**, 017007 (2001).
  - <sup>5</sup> M. Oshikawa and I. Affleck, *Phys. Rev. Lett.* **79**, 2883 (1997); *Phys. Rev. B* **60**, 1038 (1999).
  - <sup>6</sup> L. Benfatto, M. B. Silva Neto, V. Juricic, and C. Morais Smith, to appear in the *Proceedings of the International Conference on Strongly Correlated Electron Systems - SCES05*, Vienna, 2005.
  - <sup>7</sup> J. Chovan and N. Papanicolaou, *Eur. Phys. J. B* **17**, 581 (2000).
  - <sup>8</sup> L. Shekhtman, O. E. Wohlman, and A. Aharony, *Phys. Rev. Lett.* **69**, 836 (1992); W. Koshibae, Y. Ohta, and S. Maekawa, *Phys. Rev. B* **50**, 3767 (1994).
  - <sup>9</sup> K. V. Tabunshchyyk, and R. J. Gooding, *Phys. Rev. B* **71**, 214418 (2005).
  - <sup>10</sup> D. Vaknin, S. K. Sinha, D. E. Moncton, D. C. Johnston, J. M. Newsam, C. R. Safinya, and H. E. King Jr., *Phys. Rev. Lett.* **58**, 2802 (1987).
  - <sup>11</sup> T. Thio, T. R. Thurston, N. W. Preyer, P. J. Picone, M. A. Kastner, H. P. Janssen, D. R. Gabbe, C. Y. Chen and R. J. Birgeneau, and A. Aharony, *Phys. Rev. B* **38**, R905 (1988); T. Thio, and A. Aharony, *Phys. Rev. Lett.* **73**, 894 (1994).
  - <sup>12</sup> The interlayer coupling,  $J_{\perp}$ , plays also an important role for the Néel transition in  $\text{La}_2\text{CuO}_4$ . We will nevertheless proceed with our 2D model since it already captures the essential physics reported in<sup>4</sup>.
  - <sup>13</sup> V. Yu. Irkhin, and A. A. Katanin, *Phys. Rev. B* **57**, 379 (1998).
  - <sup>14</sup> B. Keimer, R. J. Birgeneau, A. Cassanho, Y. Endoh, M. Greven, M. A. Kastner, and G. Shirane, *Z. Phys. B* **91**, 373 (1993).
  - <sup>15</sup> B. Keimer, N. Belk, R. J. Birgeneau, A. Cassanho, C. Y. Chen, M. Greven, M. A. Kastner, A. Aharony, Y. Endoh, R. W. Erwin, and G. Shirane, *Phys. Rev. B* **46**, 14034 (1992).
  - <sup>16</sup> T. Nakano, M. Oda, C. Manabe, N. Momono, Y. Miura, and M. Ido, *Phys. Rev. B* **49**, 16000 (1994).
  - <sup>17</sup> In the RPA improved spin-wave analysis of<sup>9</sup>  $\chi_a(0) \sim 1/g_0c_0$  and as a consequence  $\chi_b(0) > \chi_a(0)$  is *only* obtained if  $M_a > M_c$ , in contrast to the experimental situation<sup>14</sup>.
  - <sup>18</sup> M. B. Silva Neto and L. Benfatto, cond-mat/0507103, to appear in *Phys. Rev. B* (2005).